2022 IEEE 25th International Conference on Intelligent Transportation Systems (ITSC)
October 8-12, 2022, Macau, China

Automated Driving Control of Vehicles with Guidances

Encong Sheng[1], Shuyou Yu[1], Huan Chang[1], Yajing Zhang[1], Yongfu Li[2] and Yi Hao[3]

2022 IEEE 25th International Conference on Intelligent Transportation Systems (ITSC) | 978-1-6654-6880-0/22/$31.00 ©2022 IEEE | DOI: 10.1109/ITSC55140.2022.9921780

Abstract— **Automated driving control of vehicles is considered, where both longitudinal and lateral dynamics are taken into account. Firstly, the vehicle dynamics are approximated by a global linear model obtained by Koopman operator theory. Then, a linear model predictive controller is designed, in which the global linear model is used to predict vehicle dynamics. Thus, it can reduce the computational burden accordingly. The state of the preceding vehicle is used as the reference of the following vehicle to complete the automated driving control. Finally, the efficacy of the proposed strategy is confirmed through simulation.**

I. INTRODUCTION

Connected and Automated Vehicles (CAVs) have significant advantages in improving traffic efficiency, and have attracted widespread attention. The current research on vehicle control can be divided into lateral control, longitudinal control, and lateral and longitudinal coupling control. Lateral control [1], [2] mainly refers to track a reference path by controlling the vehicle steering system. The longitudinal control [3], [4] mainly refers to the accurate control of the longitudinal velocity by controlling the driving force and braking force of vehicles. Pure longitudinal or lateral control ignores the strong coupling characteristics of vehicle lateral and longitudinal dynamics. At present, decoupling controllers [5]-[7] are often adopted in lateral and longitudinal control respectively, but they will inevitably generate system errors, making it difficult to obtain good control effects.

The vehicle is a complex coupled dynamic system with multiple inputs and multiple outputs, which needs to satisfy various dynamic constraints. Model Predictive Control (MPC) has good robustness and advantages in dealing with constraints. Thus, it has been widely used in vehicle control. Linearization is commonly used in Nonlinear Model Predictive Control (NMPC), which can effectively avoid solving nonconvex optimization problems and reduce the computational burden. However, local linearization [8] transforms the nonlinear model only near the operating point based on Taylor expansion. Multi-model method [9] is difficult to ensure the stability of model switching. Feedback linearization [10] requires precise mathematical models, and is difficult to deal with the uncertainties in the models.

The development of the Koopman operator theory [11] introduces a new idea for the linearization. Its basic idea is to linearize the nonlinear system globally without sacrificing any information by lifting it into an infinite-dimensional linear space. To apply the Koopman operator theory to practice, the infinite-dimensional Koopman operator is approximated by the data-driven Dynamic Mode Decomposition (DMD) and the Extended Dynamic Mode Decomposition (EDMD) in finite dimensions. The basic characteristics of the DMD algorithm [12] are singular value decomposition (SVD) and balanced truncation. Because of its simple mathematical expression and easy implementation, the DMD algorithm has been widely used in the analysis of complex flow phenomena. In order to apply the DMD algorithm to nonlinear controlled systems, Proctor et al. [13] proposed the algorithm of dynamic mode decomposition with control (DMDc). Studies [14]-[16] discussed the feasibility of the DMDc algorithm in different controlled systems. The EDMD algorithm [17] is an extension of the DMD algorithm. When approximating the Koopman operator, it is necessary to select the lifting functions to lift the dimension of the system' state, and the lifted state has the characteristics of linear evolution. In practical application, the selection of lifting functions is subjective, and the accuracy of the linear model based on the EDMD algorithm will be affected.

At present, researchers have tried to use the Koopman operator theory as a new idea to control the vehicles, in which the Koopman operator is used to approximate the vehicle dynamics and the controller is designed by linear control strategy. However, Cibulka et al. [18] only linearized the vehicle model and did not design a controller. The obtained linear model had limited prediction effect on vehicle state when the Koopman operator was approximated by the EDMD algorithm in [19]. Svec et al. [20] only carried out model identification and controller design for the tireless single-track vehicle model. The MPC scheme designed in [21] did not achieve good performance when the expected longitudinal velocity remained unchanged, and the expected yaw rate changed.

In this paper, an automated driving control method for vehicles based on the Koopman operator is proposed. The vehicle dynamics are approximated by the Koopman linear model identified by the DMDc algorithm, and the linear model predictive controller is designed. The preceding vehicle's

*This work is supported in part by the National Natural Science Foundation of China under Grant U1964202, in part by the Natural Science Foundation of Jilin Province under Grant YDZJ202101ZYTS169.(Corresponding author: shuyou@jlu.edu.cn)

[1]Encong Sheng, Shuyou Yu, Huan Chang, and Yajing Zhang are with the Department of Control Science and Engineering, Jilin University, Changchun, 130022, China shuyou@jlu.edu.cn, {shengec20, huanchang19, zhangyj20}@mails.jlu.edu.cn

[2]Yongfu Li is with the Department of Automation, Chongqing University of Posts and Telecommunications, Chongqing, 400065, China liyongfu@cqupt.edu.cn

[3]Yi Hao is with the Dongfeng Commercial Vehicle Technology Center, Dongfeng Motor Corporation, Wuhan, 442001, China yf-haoyi@dfcv.com.cn

Authorized licensed use limited to: JILIN UNIVERSITY. Downloaded on February 28,2023 at 13:08:01 UTC from IEEE Xplore. Restrictions apply.

state is transmitted to the following vehicle as the reference to realize the real-time control of CAVs.

The main contributions of this paper are as follows:

- When establishing the nonlinear vehicle model, the tire model working in the linear region is adopted. DMDc algorithm is used to approximate the vehicle model.
- Compared with [20] and [21], the controller designed in this paper can accurately track the yaw rate and ensure better performance under different scenarios.

This paper is organized as follows. The vehicle model is introduced in Section II. The Koopman operator theory and the DMDc algorithm for vehicle systems are introduced in Section III. The model predictive controller based on the global linear model is designed in Section IV. The simulation results are shown in Section V. Finally, the work of this paper is summarized in Section VI.

II. VEHICLE MODEL

Only the vehicle's longitudinal, lateral, and yaw motions are considered in this paper. Set the vehicle to front-wheel drive, and the vehicle dynamics model considering the lateral and longitudinal coupling is established, as shown in Fig. 1.

According to Newton's second law, the vehicle longitudinal, lateral and yaw dynamics equations [22] can be expressed as:

$$\begin{cases} m\dot{v}_x - mv_y\omega = F_{xf} + F_{xr} - C_A v_x^2 \\ m\dot{v}_y + mv_x\omega = F_{yf} + F_{yr} \\ I_z\dot{\omega} = aF_{yf} - bF_{yr} \end{cases} \tag{1}$$

where v_x, v_y and ω are the longitudinal velocity, lateral velocity and yaw rate of the vehicle, respectively, m is the mass of the vehicle, I_z is the moment of inertia around the yaw axis, a and b are distances of wheels from the center of gravity, F_{xf} and F_{yr} are the longitudinal forces of the front and rear wheels, F_{yf} and F_{yr} are the lateral forces of the front and rear wheels, and C_A is the air resistance coefficient.

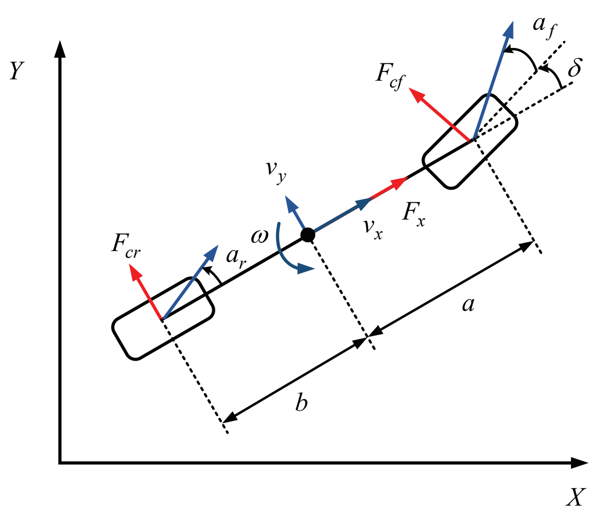

Fig. 1. Vehicle dynamics model

Assume that the tire works in the linear region. The small angle approximation method [23] is used to calculate tire force. Lateral forces of the front and rear tires are:

$$\begin{cases} F_{yf} = C_{cf}\left(\delta - \frac{v_y + a\omega}{v_x}\right) \\ F_{yr} = C_{cr}\left(\frac{b\omega - v_y}{v_x}\right) \end{cases} \tag{2}$$

where C_{cf} and C_{cr} are the cornering stiffnesses of the front and rear tires, respectively, and δ is the front steering angle. Denote $F_x = F_{xf} + F_{xr}$. Combining the above equations, the vehicle dynamics model of the lateral and longitudinal coupling is as follows:

$$\begin{cases} \dot{v}_x = v_y\omega + \frac{1}{m}\left(F_x - C_A v_x^2\right) \\ \dot{v}_y = -v_x\omega + \frac{1}{m}\left(-\frac{(C_{cf}+C_{cr})v_y}{v_x} + \frac{(C_{cr}b - C_{cf}a)\omega}{v_x} + C_{cf}\delta\right) \\ \dot{\omega} = \frac{1}{I_z}\left(-\frac{(C_{cf}a - C_{cr}b)v_y}{v_x} - \frac{(C_{cf}a^2 + C_{cr}b^2)\omega}{v_x} + C_{cf}a\delta\right) \end{cases} \tag{3}$$

Selecting the state of the system as $x = \begin{bmatrix} v_x & v_y & \omega \end{bmatrix}^T$ and the control input as $u = \begin{bmatrix} F_x & \delta \end{bmatrix}^T$, the vehicle dynamics model (3) is rewritten as:

$$\dot{x} = f(x,u) \tag{4}$$

Remark 1: The DMDc algorithm introduced in Section III for approximating the Koopman operator is data-driven. The vehicle model (3) is established to carry out the simulation experiments in Section V and construct the training dataset required by DMDc algorithm. The model itself ignores much information. When it is applied to the vehicle system in the future, the data of vehicles can be directly obtained. Thus, the data-driven, model-free method can establish the linear vehicle model.

III. KOOPMAN OPERATOR

A. Koopman Operator for Vehicle systems

The core idea of the Koopman operator theory is to express the evolution of nonlinear dynamical systems through infinite-dimensional linear operators [11]. Discretizing (4), the discrete nonlinear vehicle dynamics system is:

$$x_{k+1} = f'(x_k, u_k) \tag{5}$$

where $x_k \in \mathbb{R}^3$ and $u_k \in U \subseteq \mathbb{R}^2$ are the vehicle system' state and control input at time step k, and $f' : \mathbb{R}^3 \times \mathbb{R}^2 \to \mathbb{R}^3$ represents a nonlinear mapping.

Define κ as the infinite-dimensional Koopman operator acting on the observation function g. Under the action of κ, the nonlinear evolution of the vehicle system (5) can be transformed into a linear evolution:

$$\kappa g(x_k) = g(x_{k+1}) = g\left(f'(x_k, u_k)\right) \tag{6}$$

Authorized licensed use limited to: JILIN UNIVERSITY. Downloaded on February 28,2023 at 13:08:01 UTC from IEEE Xplore. Restrictions apply.

B. DMDc Algorithm

The traditional DMD algorithm is only suitable for describing autonomous systems. To eliminate this limitation, the DMDc algorithm [13] extends the traditional DMD algorithm to controlled systems. This subsection will complete the construction of the global linear model based on the DMDc algorithm.

Based on the DMDc algorithm, the vehicle nonlinear system (5) can be expressed as the discrete linear controlled model:

$$\begin{cases} \hat{x}_{k+1} = A_{DMD}\hat{x}_k + B_{DMD}u_k \\ \hat{y}_k = C_{DMD}\hat{x}_k \end{cases} \tag{7}$$

where $\hat{x}_k \in \mathbb{R}^3$ and $\hat{y}_k \in \mathbb{R}^3$ are the state and output of the constructed linear model, respectively, the matrix C_{DMD} is set to $I_{3\times3}$, and the matrices $A_{DMD} \in \mathbb{R}^{3\times3}$ and $B_{DMD} \in \mathbb{R}^{3\times2}$ are the parameter matrices that need to be identified.

The DMDc algorithm is a data-driven algorithm. To identify the matrices A_{DMD} and B_{DMD}, the input and output data of the vehicle nonlinear system are first collected, and the following data matrix is constructed:

$$\begin{aligned} X &= [x_1, \cdots, x_{k_{\max}}] \\ Y &= [x_2, \cdots, x_{k_{\max}+1}] \\ U &= [u_1, \cdots, u_{k_{\max}}] \end{aligned} \tag{8}$$

where X and Y are the data matrices formed by the states of the vehicle sysytem (5) at the adjacent moment, U is the data matrix formed by the control input, and k_{max} is the number of snapshots.

According to the Koopman linear model (7), the matrix Y can be expressed as:

$$Y = \begin{bmatrix} A_{DMD} & B_{DMD} \end{bmatrix} \begin{bmatrix} X \\ U \end{bmatrix} = G\Omega \tag{9}$$

where $G = \begin{bmatrix} A_{DMD} & B_{DMD} \end{bmatrix}$ is the finite-dimensional approximate matrix of the Koopman operator, and $\Omega = \begin{bmatrix} X & U \end{bmatrix}^T$ is the reconstructed augmented data matrix.

Perform singular value decomposition(SVD) on the matrix Ω, and define the truncated rank of SVD as p. The dimension of the vehicle model (5) established in this paper is relatively low, so p is set to 3. The matrix Ω can be expressed as:

$$\Omega \approx \tilde{U}\tilde{\Sigma}\tilde{V}^T \tag{10}$$

where $\tilde{U} \in \mathbb{R}^{5\times3}$ is the unitary matrix, and $\tilde{\Sigma} \in \mathbb{R}^{3\times3}$ is the diagonal matrix.

To get the matrices A_{DMD} and B_{DMD} from the matrix G, decompose the matrix $\tilde{U}$, we can get:

$$\tilde{U} = \begin{bmatrix} \tilde{U}_1 \\ \tilde{U}_2 \end{bmatrix} \tag{11}$$

where $\tilde{U}_1 \in \mathbb{R}^{3\times3}$ and $\tilde{U}_2 \in \mathbb{R}^{2\times3}$.

The matrices A_{DMD} and B_{DMD} in the Koopman linear model can be expressed as:

$$\begin{aligned} A_{DMD} &= Y\tilde{V}\tilde{\Sigma}^{-1}\tilde{U}_1^T \\ B_{DMD} &= Y\tilde{V}\tilde{\Sigma}^{-1}\tilde{U}_2^T \end{aligned} \tag{12}$$

The finite-dimensional approximation of the Koopman operator using the DMDc algorithm is summarized in Algorithm 1.

Algorithm 1 Approximation of Koopman operator with the DMDc algorithm

1) Collect the input and output data of nonlinear vehicle systems, and construct the following data matrices:

$$\begin{aligned} X &= [x_1, \cdots, x_{k_{\max}}] \\ Y &= [x_2, \cdots, x_{k_{\max}+1}] \\ U &= [u_1, \cdots, u_{k_{\max}}] \end{aligned}$$

2) Construct the augmented matrix Ω:

$$\Omega = \begin{bmatrix} X & U \end{bmatrix}^T$$

3) Perform singular value decomposition(SVD) on matrix Ω

$$\Omega \approx \tilde{U}\tilde{\Sigma}\tilde{V}^T$$

4) Decompose the matrix $\tilde{U}$ into $\tilde{U}_1$ and $\tilde{U}_2$, and calculate the matrices A_{DMD}, B_{DMD}.

$$\begin{aligned} A_{DMD} &= Y\tilde{V}\tilde{\Sigma}^{-1}\tilde{U}_1^T \\ B_{DMD} &= Y\tilde{V}\tilde{\Sigma}^{-1}\tilde{U}_2^T \end{aligned}$$

IV. CONTROLLER DESIGN

The vehicle system is a nonlinear system with strong coupling characteristics. In this paper, the identified Koopman linear model is used to design a linear model predictive controller, which takes the velocity information of the preceding vehicle as the reference of the following vehicle. The MPC algorithm based on Koopman operator is summarized in Algorithm 2, and the control system's framework is shown in Fig. 2.

The optimization problem of the linear model predictive controller designed in this paper is as follows:

Problem 1.

$$\underset{U_k}{minimize}\, J(\hat{x}_k, r_k, U_k) \tag{13}$$

s.t.

$$\begin{aligned} &\hat{x}_{k+i+1|k} = A_{DMD}\hat{x}_{k+i|k} + B_{DMD}u_{k+i|k} \\ &\hat{y}_{k+i|k} = C_{DMD}\hat{x}_{k+i|k} \\ &\hat{x}_{k|k} = x_k \\ &\hat{x}_{k+i|k} \in [\hat{x}_{min}, \hat{x}_{max}] \\ &u_{k+i|k} \in [u_{min}, u_{max}] \end{aligned} \tag{14}$$

where $\hat{x}_{k+i|k}$ and $\hat{y}_{k+i|k}$ are the predicted state and predicted output based on the Koopman linear model, respectively, N is the prediction horizon, $U_k = [u_{k|k}, u_{k+1|k}, \ldots, u_{k+N-1|k}]$ is the sequence of the control input, $r_k = [r_{k|k}, r_{k+1|k}, \ldots, r_{k+N-1|k}]$ is the reference sequence, Q and R are positive semi-definite weight matrices, $\hat{x}_{min/max}$ and $u_{min/max}$ are constraints of the

Algorithm 2 MPC Based on the Koopman Operator

1: **for** $k = 0, 1, \ldots$ **do**
2: Obtain the current state x_k of the vehicle system
3: Obtain the state $\hat{x}_{k|k}$ of the Koopman linear model
4: Solve Problem 1, and obtain $\mathbf{U}_k^*$
5: Apply $u_{k|k}^*$ to the vehicle system

Authorized licensed use limited to: JILIN UNIVERSITY. Downloaded on February 28,2023 at 13:08:01 UTC from IEEE Xplore. Restrictions apply.

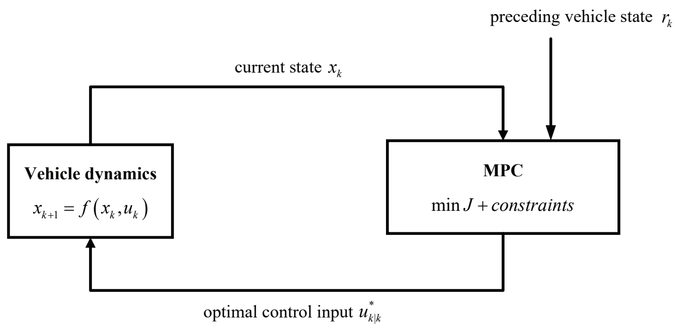

Fig. 2. Control block diagram of model predictive controller based on Koopman operator

system state and control input, and the cost function is as follows:

$$J(\hat{x}_k, r_k, U_k) = \sum_{i=0}^{N-1} \left[\left\| \hat{y}_{k+i|k} - r_{k+i|k} \right\|_Q^2 + \left\| u_{k+i|k} \right\|_R^2 \right] \quad (15)$$

Denote $U_k^* = \left[u^*_{k|k}, u^*_{k+1|k}, \ldots, u^*_{k+N-1|k} \right]$ and $J^*\left(\hat{x}_k, r_k, U_k^*\right)$ as the optimal control sequence and the related optimal cost function. Apply the first element of U_k^*, i.e., $u^*_{k|k}$ to the following vehicle.

V. SIMULATION RESULTS

To evaluate the efficiency of the global linear model and the designed linear model predictive controller, simulation experiments under different driving scenarios are performed in the Matlab R2016b environment. The Koopman linear model, which can approximate vehicle dynamics, is identified based on the DMDc algorithm. The parameters of the vehicle model in this paper are shown in Table I.

A. Data Collection and Model Identification

The data of the vehicle system must first be collected before utilizing the DMDc algorithm to construct the Koopman linear model. Set the sampling period T_s to $10ms$, and use the Runge-Kutta method to discretize (4). Select 2000 trajectories with the time scale of 200 steps to form the dataset. To obtain data that can accurately reflect the traits of vehicles, the number of trajectories in the dataset is divided equally to form the straight driving subdataset and the curve driving subdataset, respectively. The settings of the two subdatasets are as follows:

- *Straight driving subdataset:* The initial values of longitudinal velocity v_x, lateral velocity v_y, and yaw rate ω are randomly selected in $[1,30]\,m/s$, $[-0.5,0.5]\,m/s$, and $[-0.5,0.5]\,rad/s$. The longitudinal force F_x is randomly selected in $[-5000,5000]\,N$, and the front steering angle δ is randomly selected in $[-0.001,0.001]\,rad$.
- *Curve driving subdataset:* The initial values of longitudinal velocity v_x, lateral velocity v_y, and yaw rate ω are randomly selected in $[1,30]\,m/s$, $[-2,2]\,m/s$, and $[-2,2]\,rad/s$. The longitudinal force F_x is randomly selected in $[-5000,5000]\,N$, and the front steering angle δ is randomly selected in $[-1,1]\,rad$.

TABLE I
VEHICLE PARAMETERS

Parameter	Value	Unit
C_A	1.12	–
m	1024	kg
g	9.8	m/s^2
I_z	3216	$kg \cdot m^2$
a	1.04	m
b	1.28	m
C_{cf}	66900	N/rad
C_{cr}	62700	N/rad

B. Model Validation

To analyze the performance of the identified Koopman linear model, simulation experiments are carried out under scenario 1 and 2 to compare the states of the linear system constructed by the Koopman operator and the actual vehicle system. The two scenarios are set as follows:

- *Scenario 1 (longitudinal motion):* The initial state of the vehicle system is set to $\begin{bmatrix} 20 & 0 & 0 \end{bmatrix}^T$, the longitudinal force F_x is set to $2000N$, and the front steering angle δ is set to 0.
- *Scenario 2 (lateral and longitudinal coupling motion):* The initial state of the vehicle system is set to $\begin{bmatrix} 20 & 0.5 & -0.35 \end{bmatrix}^T$, the longitudinal force F_x is set to $-2000N$, and the front steering angle satisfies $\delta = 0.1\sin(0.4\pi t)$.

To objectively reflect the established Koopman linear model's accuracy, the Root Mean Square Error (RMSE) is used as an objective evaluation index, i.e.,

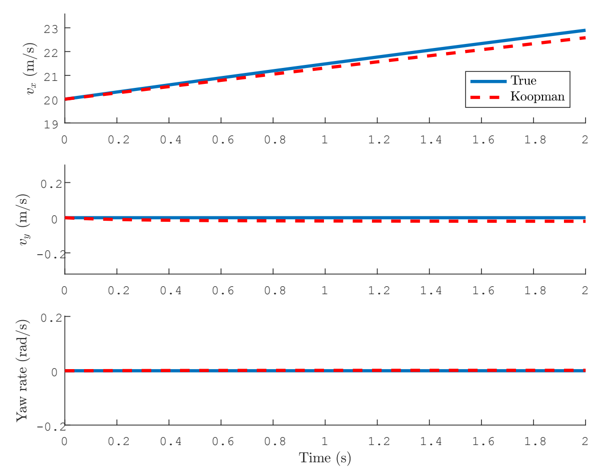

Fig. 3. Prediction results of longitudinal and lateral velocity and yaw rate (Scenario 1)

Authorized licensed use limited to: JILIN UNIVERSITY. Downloaded on February 28,2023 at 13:08:01 UTC from IEEE Xplore. Restrictions apply.

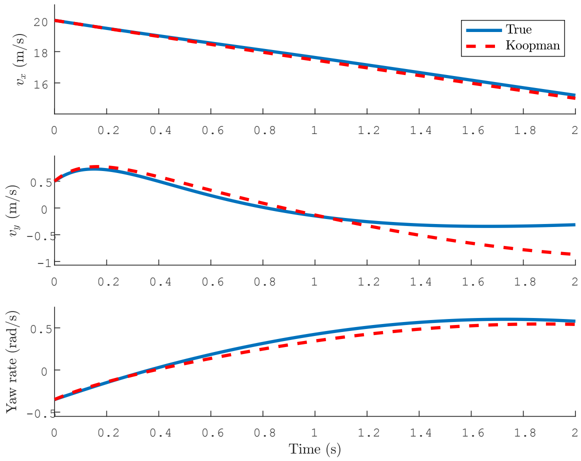

Fig. 4. Prediction results of longitudinal and lateral velocity and yaw rate (Scenario 2)

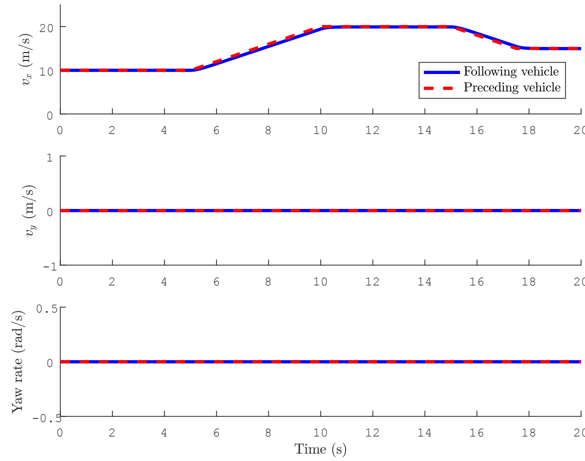

Fig. 5. Control effect of vehicle controller (Control scenario 1)

$$RMSE = \frac{\sqrt{\sum_k \left\| x_{pred}(k) - x_{true}(k) \right\|_2^2}}{\sqrt{\sum_k \left\| x_{true}(k) \right\|_2^2}} \times 100\% \tag{16}$$

where $x_{pred}(k)$ and $x_{true}(k)$ are the state estimation based on the global linear model at time step k and the actual vehicle system state, respectively.

Fig. 3 and Fig. 4 are the simulation results under two scenarios. The RMSE under the two scenarios are 0.89% and 1.57%, respectively. The global linear model obtained by the Koopman operator can accurately approximate the vehicle dynamics.

C. Automated driving with guidances

Simulation experiments are performed in different scenarios to confirm the effectiveness of the designed model predictive controller. The two control scenarios are set as follows:

- *Control scenario 1:* Set the expected values of lateral velocity v_y and yaw rate ω to 0, and the longitudinal velocity v_x is constantly changing.
- *Control scenario 2:* Set the longitudinal velocity v_x as a fixed value, and the expected values of the lateral velocity v_y and yaw rate ω are constantly changing.

Remark 2: It is assumed in control scenario 1 and 2 that the state of the preceding vehicle (i.e., the desired state) and the following vehicle are identical at the initial moment. When the state of the preceding vehicle changes, the state of the following vehicle changes accordingly.

Set the prediction horizon N to 10. The constraints of v_x, v_y and ω are $[-35,35]\, m/s$, $[-1,1]\, m/s$, and $[-1,1]\, rad/s$. The constraints of the longitudinal force F_x and the front steering angle δ are $[-5000,5000]\, N$ and $[-1,1]\, rad$. The weight matrices are set as follows:

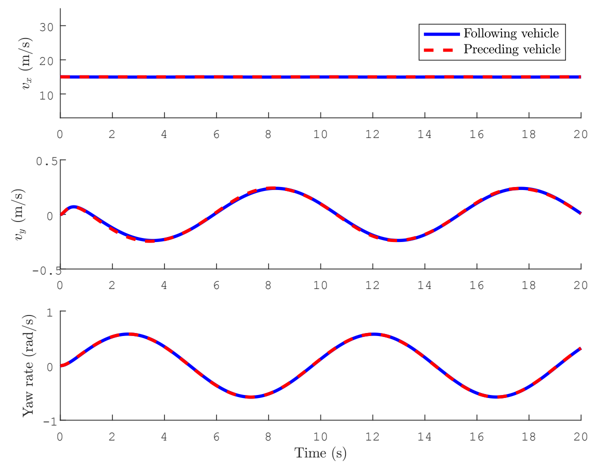

Fig. 6. Control effect of vehicle controller (Control scenario 2)

$$\begin{aligned} Q &= \begin{bmatrix} 50000 & 0 & 0 \\ 0 & 5000 & 0 \\ 0 & 0 & 500000 \end{bmatrix} \\ R &= \begin{bmatrix} 0.001 & 0 \\ 0 & 0.1 \end{bmatrix} \end{aligned} \tag{17}$$

Control scenario 1 simulates vehicles driving longitudinally with variable velocity. Fig. 5 shows that the following vehicle can accurately track the desired longitudinal velocity and ensure that the lateral velocity and yaw rate are close to zero.

Control scenario 2 simulates the steering and lane changing scenarios of vehicles. The designed model predictive controller can quickly and effectively track the preceding vehicle's changing lateral velocity and yaw rate, as shown in Fig. 6.

The processor model is Intel(R)Core(TM) i7-10700CPU @2.90 GHz, and the RAM is 16GB. The optimization problem in this paper is solved by qpOASES [24]. The

Authorized licensed use limited to: JILIN UNIVERSITY. Downloaded on February 28,2023 at 13:08:01 UTC from IEEE Xplore. Restrictions apply.

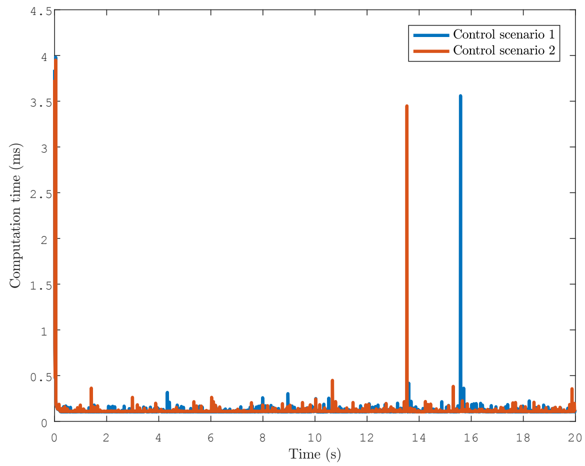

Fig. 7. Computation time of optimization problem

computation time of the optimization problem of the control scenario 1 and 2 is shown in Fig. 7. The average computation time is 0.117 ms and 0.120 ms, respectively.

VI. CONCLUSION

In this paper, data-driven model identification and control strategy based on the Koopman linear model identified by the DMDc algorithm is applied to the vehicle system. The vehicle dynamics whose tires work in the linear region are approximated by the Koopman linear model. Simulation experiments under different driving scenarios verify the effectiveness of the DMDc algorithm in the application of vehicle models. The linear model predictive controller is designed based on the Koopman linear model, which avoids the solution of nonconvex optimization problems and reduces the computational burden accordingly.

REFERENCES

[1] F. Y. Wang, Q. N. Xu, S. He, and J. Zhong, "Research on Lateral Control Strategy of Intelligent Electrical Vehicle" *Machinery Design and Manufacture*, no. 04, pp. 224-227, 2018.

[2] S. Mata, A. Zubizarreta, and I. Cabanes, "Linear time varying model based model predictive control for lateral path tracking," *International Journal of Vehicle Design*, vol. 75, no. 1-4, pp. 1-22, 2018.

[3] A. Raffin, M. Taragna, and M. Giorelli, "Adaptive longitudinal control of an autonomous vehicle with an approximate knowledge of its parameters," in *2017 11th International Workshop on Robot Motion and Control (RoMoCo)*. 2017, pp. 1-6.

[4] J. H. Guo, L. H. Li, P. Hu, and M. H. Zhang, "Longitudinal Multiple Sliding-mode Control of Unmanned Vehicle via Fuzzy Logic," *China Journal of Highway and Transport*, vol. 26, no. 01, pp. 170-176, 2013.

[5] S. Chen, G. Xiong, H. Chen, and D. Negrut, "MPC-based path tracking with PID speed control for high-speed autonomous vehicles considering time-optimal travel," *Journal of Central South University*, vol. 27, no. 12, pp. 3702-3720, 2020.

[6] H. Xie, and S.S.Liu, "Lateral and longitudinal motion control of unmanned vehicles using model predictive control," *Journal of Automotive Safety and Energy*, vol. 10, no. 03, pp. 326-333, 2019.

[7] T. Deng, and X. Li, "Combined Control Method of Intelligent Vehicle Longitudinal and Lateral Motion," *Journal of Chongqing Jiaotong University (Natural Science)*, vol. 40, no. 04, pp. 133-140, 2021.

[8] H. F. Shi, M. C. Liu, and J. H. Huang, "Lateral and longitudinal motion cooperative control of intelligent electric vehicle," *Journal of Nanchang University (Engineering and Technology)*, vol. 43, no. 01, pp. 62-72, 2021.

[9] P. Wang, S. Y. Li, "Multiple mode-based predictive control for a class of nonlinear systems," *Control and Decision*, no. 10, pp. 1113-1118, 2007.

[10] S. Quan, Y. X. Wang, X. Xiao, H. He, and F. Sun, "Feedback linearization-based MIMO model predictive control with defined pseudo-reference for hydrogen regulation of automotive fuel cells," *Applied Energy*, vol. 293, p. 116919, 2021.

[11] B. O. Koopman, "Hamiltonian Systems and Transformation in Hilbert Space," *Proceedings of the National Academy of Sciences*, vol. 17, no. 05, pp. 315-318, 1931.

[12] P. J. Schmid, "Dynamic mode decomposition of numerical and experimental data," *J. Fluid Mech*, vol. 656, pp. 5-28, 2010.

[13] J. L. Proctor, S. L. Brunton, and J. N. Kutz, "Dynamic Mode Decomposition with Control," *SIAM Journal on Applied Dynamical Systems*, vol. 15, no. 1, pp. 142-161, 2016.

[14] A. Narasingam and J. S.-I. Kwon, "Development of local dynamic mode decomposition with control: Application to model predictive control of hydraulic fracturing," *Computers & Chemical Engineering*, vol. 106, pp. 501-511, 2017.

[15] Q. Lu, S. Shin, and V. M. Zavala, "Characterizing the Predictive Accuracy of Dynamic Mode Decomposition for Data-Driven Control," in *IFAC-PapersOnLine*, vol. 53, no. 2, pp. 11289-11294, 2020.

[16] B. Swaminathan, J. G. Manathara, and A. K. Vinayagam, "Application of Dynamic Mode Decomposition with Control (DMDc) for aircraft parameter estimation," *IFAC-PapersOnLine*, vol. 55, no. 1, pp. 789-794, 2022.

[17] M. O. Williams, I. G. Kevrekidis, and C. W. Rowley, "A Data-Driven Approximation of the Koopman Operator: Extending Dynamic Mode Decomposition," *J Nonlinear Sci*, vol. 25, no. 6, pp. 1307-1346, 2015.

[18] V. Cibulka, T. Hani, and M. Hromk, "Data-driven identification of vehicle dynamics using Koopman operator," in *2019 22nd International Conference on Process Control (PC19)*. 2019, pp. 167-172.

[19] Y. Xiao, X. Zhang, X. Xu, X. Liu, and J. Liu, "Deep Neural Networks with Koopman Operators for Modeling and Control of Autonomous Vehicles," *arXiv:2007.02219*, 2022.

[20] M. Svec, S. Iles, and J. Matusko, "Model predictive control of vehicle dynamics based on the Koopman operator with extended dynamic mode decomposition," in *2021 22nd IEEE International Conference on Industrial Technology (ICIT)*. 2021, pp. 68-73.

[21] V. Cibulka, M. Korda, T. Hani, and M. Hromk, "Model Predictive Control of a Vehicle using Koopman Operator," *arXiv:2103.04978*, 2022.

[22] R. Rajamani, "Longitudinal control for vehicle platoons," in *Vehicle Dynamics and Control*, 2th ed. Boston, MA, USA: Springer, 2012, pp. 15-45.

[23] C. Bian, G. Yin, N. Zhang, and L. Xu, "Takagi-sugeno fuzzy model predictive controller design for combining lane keeping and speed tracking of four wheels steering and four wheels drive electric vehicle," in *2017 29th Chinese Control And Decision Conference (CCDC)*. 2017, pp. 4067-4072.

[24] H. J. Ferreau, C. Kirches, A. Potschka, H. G. Bock, and M. Diehl, "qpOASES: a parametric active-set algorithm forquadratic programming," *Mathematical Programming Computation*, vol. 6, no. 4, pp. 327-363, 2014.

Authorized licensed use limited to: JILIN UNIVERSITY. Downloaded on February 28,2023 at 13:08:01 UTC from IEEE Xplore. Restrictions apply.